tint persisted. After the solution was allowed to warm to 0 °C, the solvent was removed under reduced pressure. Purification of the crude product by MPLC (SiO_2, 20:1 chloroform/methanol) afforded 33 mg (88% yield) of *cis*-**5** as a brittle white foam: mp 134–136 °C dec; ^{31}P NMR (32.2 MHz, acetone-d_6) δ −13.6; ^1H NMR (300 MHz, acetone-d_6) δ 7.55 (br s, 1 H, H_4), 7.22–7.49 (m, 5 H, C_6H_5), 6.43 (dd, 1 H, $H_{1'}$), 5.24 (apparent q, 1 H, $H_{3'}$), 4.63–4.79 (m, 2 H, $H_{5'a}$, and $H_{5'b}$), 4.05–4.13 (m, 1 H, $H_{4'}$), 2.65–2.78 (m, 2 H, $H_{2'a}$, and $H_{2'b}$), 1.81 (d, 3 H, 5-Me, J_{HH} = 1.2 Hz).

***cis*-Thymidine 3′,5′-Cyclic Phenyl Phosphite, 9.** Phosphoramidite **8** (250 mg, 0.83 mmol) was dissolved in 20 mL of stirred methylene chloride under a dry CO_2 atmosphere. A few crystals of dimethylamine hydrochloride were added. After 24 h phenol (86 mg, 0.91 mmol) was added followed by further stirring for 24 h under CO_2. Solvent removal in vacuo yielded crude **2** as a pale yellow brittle foam, which on purification by MPLC (SiO_2, 20:1 chloroform/methanol) yielded 89 mg (36% yield) of **9** as the cis diastereomer, a brittle white foam: ^{31}P NMR (32.2 MHz, acetone-d_6) δ 115.0; ^1H NMR (300 MHz, acetone-d_6) δ 7.54 (br s, 1 H, H_4), 7.0–7.2 (m, 5 H, C_6H_5), 6.28 (dd, 1 H, $H_{1'}$), 4.92–5.02 (m, 1 H, $H_{3'}$), 4.71 (ddd, 1 H, $H_{5'a}$), 4.43 (ddd, 1 H, $H_{5'b}$), 3.80 (7, 1 H, $H_{4'}$), 2.51–2.58 (m, 2 H, $H_{2'a}$ and $H_{2'b}$), 1.81 (d, 3 H, 5-Me, J_{HH} = 1.2 Hz).

Collection and Reduction of X-ray Data. Crystals of *trans*-**5**, suitable for X-ray diffraction, were obtained by vapor diffusion of hexane into a solution of the compound in ethyl acetate. A well-formed crystal was mounted on a Syntex $P\bar{1}$ auto diffractometer equipped with scintillation counter and graphite monochromated Mo Kα radiation. The cell dimensions (Table IV) were obtained by a least-squares fit of 2θ settings of 15 reflections. The data were reduced to F_o and $\sigma(F_o)$. Lorentz and polarization corrections were applied to all reflections.

Solution and Refinement of Structure. The structure was solved by direct methods and was refined by full-matrix least-squares technique[25] by using neutral atom scattering factors[26] for all species. Hydrogen atoms were added in geometrically ideal positions. Anisotropic refinement converged at

$$R = \sum||F_o| - |F_c||/\sum|F_o| = 0.053$$

and

$$R_w = \sum w^{1/2}|F_o - F_c|/\sum w^{1/2}|F_o| = 0.061$$

The weighting scheme was given by $w = 0.2814[\sigma^2(F_o) + 0.006F_o^2]^{-1}$. The final atomic parameters with their standard deviations are given in Table V.

Acknowledgment. This work was supported by Grant CA 11045 from the National Cancer Institute of the Public Health Service.

Registry No. *trans*-**5**, 108146-35-6; *cis*-**5**, 108146-36-7; *trans*-**8**, 66512-19-4; *cis*-**9**, 87970-09-0; **11**, 108060-82-8; PhONa, 139-02-6; *o*-$NO_2C_6H_4OH$, 88-75-5; $(Me_2N)_3P$, 1608-26-0; PhOH, 108-95-2; thymidine, 50-89-5.

Supplementary Material Available: Tables of hydrogen atom parameters, atomic thermal parameters, bond lengths, bond angles, and torsion angles (7 pages); table of structure factors (13 pages). Ordering information is given on any current masthead page.

(24) Drew, M. G. B.; Rodgers, J.; White, D. W.; Verkade, J. G. *Chem. Commun.* **1971**, 227.
(25) All calculations were performed with the SHELXTL program system written by G. M. Sheldrick.
(26) *International Tables for X-ray Crystallography*; Kynoch Press: Birmingham, England, 1974; Vol. IV, pp 72–98.1.

Cu(II) Coordination Chemistry of Amine Oxidases: Pulsed EPR Studies of Histidine Imidazole, Water, and Exogenous Ligand Coordination

John McCracken,[1a] Jack Peisach,[1a] and David M. Dooley*[1b]

Contribution from the Department of Molecular Pharmacology, Albert Einstein College of Medicine, Yeshiva University, Bronx, New York 10461, and the Department of Chemistry, Amherst College, Amherst, Massachusetts 01002. *Received October 10, 1986*

Abstract: Pulsed EPR spectroscopy utilizing the electron spin echo envelope modulation technique was used to study the Cu(II) binding sites in porcine kidney and bovine plasma amine oxidases. For both proteins, two magnetically distinct histidyl imidazoles were identified as Cu(II) ligands. The assignment of water as another metal ligand is based on comparison with echo envelope data for a series of copper(II)-bipyridyl complexes where the individual effects of axial, equatorial, and ambient water can be differentiated. Anionic inhibitors of amine oxidases, such as cyanide and azide, are shown to bind directly to Cu(II), displacing equatorially bound water. Once these anions are bound, the distinction in magnetic coupling between the two populations of imidazoles is lost.

In recent years, considerable progress has been made toward understanding the active site structures and mechanisms of copper-containing amine oxidases. In addition to metal ions, these metalloenzymes also contain a covalently bound organic cofactor, believed to be methoxatin, pyrrolloquinolinequinone (PQQ) or a close analogue.[2,3] Two copper ions are bound per enzyme molecule, which is generally composed of two subunits with a total molecular weight of approximately 180000.[4,5] At least one copper and a single PQQ are required for enzyme activity,[4-9] which is to catalyze the two-electron oxidative deamination of primary

(1) (a) Albert Einstein College of Medicine. (b) Amherst College.
(2) (a) Lobenstein-Verbeek, C. L.; Jongejan, J. A.; Frank, J.; Duine, J. A. *FEBS Lett.* **1984**, *170*, 305–309. (b) Ameyama, M.; Hayashi, M.; Matsushita, K.; Shinagawa, E.; Adachi, O. *Agric. Biol. Chem.* **1984**, *48*, 561–565.
(3) (a) Moog, R. S.; McGuirl, M. A.; Cote, C. E.; Dooley, D. M. *Proc. Natl. Acad. Sci. U.S.A.* **1986**, *83*, 8435–8439. (b) Knowles, P. F.; Pandeya, K. B.; Rius, F. X.; Spencer, C. M.; Moog, R. S.; McGuirl, M. A.; Dooley, D. M. *Biochem. J.* **1987**, *241*, 603–608.
(4) Knowles, P. F.; Yadav, K. D. S. In *Copper Proteins and Copper Enzymes*; Lontie, R., Ed.; CRC Press: Boca Raton, FL, 1984; Vol. 2, pp 103–129.
(5) *Structure and Functions of Amine Oxidases*; Mondovi, B., Ed.; CRC Press: Boca Raton, FL, 1985.
(6) Mondovi, B.; Sabatini, S.; Befani, O. *J. Mol. Catal.* **1984**, *23*, 325–330.
(7) Suzuki, S.; Sakurai, T.; Nakahara, A.; Manabe, T.; Okuyama, T. *Biochemistry* **1986**, *25*, 338–341.
(8) Grant, J.; Kelly, I.; Knowles, P. F.; Olsson, J.; Pettersson, G. *Biochem. Biophys. Res. Commun.* **1978**, *83*, 1216–1224.
(9) Rotilio, G. In *Structure and Functions of Amines Oxidases*; Mondovi, B., Ed.; CRC Press: Boca Raton, FL, 1985, pp 127–134, and references cited therein.

0002-7863/87/1509-4064$01.50/0

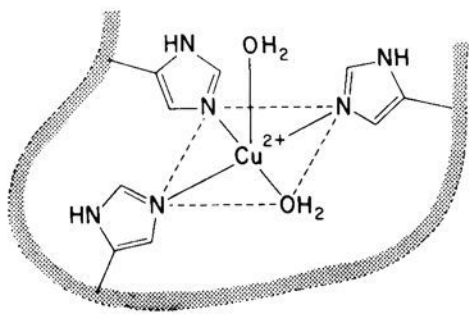

Figure 1. Proposed structure for the Cu(II) site of amine oxidases.

amines, (eq 1–3). Here, E and E_{red} are the oxidized and reduced forms of the enzyme, respectively.

$$E + RCH_2NH_2 \rightarrow E{\cdot}RCH_2NH_2 \rightarrow E_{red} + RCHO \quad (1)$$

$$E_{red} + O_2 + H_2O \rightarrow E + NH_3 + H_2O_2 \quad (2)$$

$$RCH_2NH_2 + O_2 + H_2O \rightarrow RCHO + NH_3 + H_2O_2 \quad (3)$$

A preliminary model for the Cu(II) site structure in amine oxidases, suggested from X-ray absorption spectroscopy (XAS) and other spectroscopic and chemical data, is shown in Figure 1. (In all of these studies, both Cu(II) binding sites are considered to have the same structure.) The X-ray absorption edge and EXAFS data are consistent with 3–4 equatorial imidazole-like ligands bound to copper,[10] while solvent ^1H NMR relaxation and ENDOR measurements suggest coordinated water in both equatorial and axial positions.[11,12]

Several anions, e.g., N_3^-, SCN^-, CN^-, are catalytic inhibitors and are known to bind to enzyme Cu(II).[11-15] It has been suggested that coordinated H_2O is the leaving group when anions such as CN^- bind, yet this does not greatly reduce the solvent ^1H *relaxation rate even though the EPR spectrum is markedly* changed, suggesting alteration of Cu(II) ligation.[11] Furthermore, the thermodynamics for N_3^- and SCN^- binding to the bovine plasma enzyme and to a chemical model Cu^{II}dien, where H_2O is the leaving group when anions bind, are markedly different.[16] Therefore, an independent method for examining alterations at the Cu(II) binding site when anions are ligated to the metal is required. As several anions inhibit amine oxidases, mechanistic information on the role of copper in the reaction may be obtained by comparing the structural and kinetic consequences of anion binding. More generally, exogenous ligands can provide useful probes of the structure and reactivity of the copper sites.

Pulsed EPR spectroscopy has developed into a powerful and versatile technique for studying the structure of paramagnetic metalloproteins.[17] Electron spin echo (ESE) envelope modulation measurements have been used to characterize imidazole coordination,[18] exogenous ligand binding,[18d-f] substrate (or substrate analogue) binding,[19] and the accessibility of metal ions to solvent H_2O.[20] This present paper describes ESE results on resting (oxidized) bovine plasma and porcine kidney amine oxidases and their complexes with azide and cyanide. For both proteins, we find two kinds of magnetically inequivalent imidazoles coordinated to Cu(II). Anion addition does not replace the imidazoles but does perturb their coupling to the metal ion. Theoretical simulations of ESE modulation envelopes as well as comparisons with modulations obtained for $Cu^{II}(bipyridyl)_n(H_2O)_{6-2n}$ model complexes indicate that H_2O is bound to Cu(II) in both amine oxidases studied. Anions displace that tightly bound H_2O having magnetic coupling parameters similar to those found for equatorially bound water in the $Cu^{II}(bipy)(H_2O)_4$ complex. Our results are also consistent with the view that water, more weakly bound than that displaced upon anion addition, remains bound to Cu(II).

Experimental Section

A block diagram of the pulsed EPR instrument used in this study is shown in Figure 2. The microwave bridge, operating from 8 to 18 GHz, consists of three major sections: the microwave pulse transmitter, the sample cavity, and the microwave receiver. Microwave pulses are generated by pulse modulating a phase-locked, cw klystron (Varian Model X-13 or X-12) with a fast PIN diode switch (MA/COM Model 8430-177). The low power output pulses are then passed through a 0°/180° phase modulator (General Microwave Model F1938) and a coaxial attenuator and are then amplified to the level of approximately 1 kW by a pulsed traveling wave tube (Space Microwave Laboratories Model 6001). The high power pulses are then passed through a rotary vane attenuator (Hewlett-Packard Model X382A or P382A) and delivered to the sample cavity.

Two different microwave cavity systems were used in these measurements. For protein samples, a stripline transmission cavity identical with that developed by Mims was utilized.[21] For studies on $Cu^{II}(bipyridyl)_n$ model compounds (see below), a second cavity system employing a folded stripline as the resonant element[22] and a cavity header assembly designed by Britt and Klein[23] was used. The latter cavity system offers several advantages over the former in that coupling to the resonator can be varied, the sample is held in a conventional 4-mm o.d. EPR tube, and the sample can be changed from the top of the dewar without removing the header assembly from the liquid He bath.

The microwave receiver uses a double-balanced mixer as a detection element (RHG Model DM1-18AB) in a homodyne arrangement. Pulsed radiation from the sample cavity is either amplified or limited by a continuous wave (cw), low noise, travelling wave tube (Watkins Johnson Model WJ-491 or WJ-307). A second PIN diode switch is used in the receiver to attenuate the mixer input during microwave pulsing. After detection, spin echoes are amplified and sampled by a two channel gated integrator (Computerware Interface Technology).

The collection of ESE envelopes is controlled by an Apple II-plus computer. This task is accomplished via control of four components: a programmable clock, used to control the overall repetition rate of the ESE pulse sequences; three digital delay generators with 1-ns resolution (Berkeley Nucleonics Corporation Model 7085), used to generate the accurate delays needed to control microwave pulse spacings and initiate spin echo integration; a dual channel gated integrator, used to measure echo intensity; and an X–Y plotter, used to display the recorded spin echo envelope during data collection. After data have been collected by the Apple computer, they are transferred to an LSI 11/73 based laboratory computer for analyses.

Both two pulse (90°–τ–180°) and stimulated echo sequences (90°–τ–90°–T–90°)[24] were used in this study. For two pulse experiments, τ was varied from 120 ns to 2 μs for each data set containing 1024 points. Stimulated echo envelope data were collected over a time range of τ + 80 ns to approximately 15 μs. Measurement conditions were as follows: microwave frequency, approximately 9.5 GHz; magnetic field strength, 3300 G; microwave pulse power, 20–50 W; pulse width, 20 ns (FWHM); temperature, 4.2 K; and pulse repetition rate, 100 Hz.

(10) Scott, R. A.; Dooley, D. M. *J. Am. Chem. Soc.* **1985**, *107*, 4348–4350.
(11) (a) Barker, R.; Boden, N.; Cayley, G.; Charlton, S. C.; Henson, R.; Holmes, M. C.; Kelly, I. D.; Knowles, P. F. *Biochem. J.* **1979**, *177*, 289–302. (b) Dooley, D. M.; McGuirl, M. A.; Koenig, S., unpublished observations.
(12) Baker, G. J.; Knowles, P. F.; Pandeya, K. B.; Rayner, J. B. *Biochem. J.* **1986**, *237*, 609–612.
(13) Dooley, D. M.; Cote, C. E. *Inorg. Chem.* **1985**, *24*, 3996–4000.
(14) (a) Dooley, D. M.; Golnik, K. C. *J. Biol. Chem.* **1983**, *258*, 4245–4248. (b) Dooley, D. M.; McGuirl, M. A. *Inorg. Chim. Acta* **1986**, *123*, 231–236. (c) Dooley, D. M.; Cote, C. E.; Golnik, K. C. *J. Mol. Catal.* **1984**, *23*, 243–253.
(15) (a) Lindstrom, A.; Olsson, B.; Pettersson, G. *Eur. J. Biochem.* **1974**, *48*, 237–243. (b) Olsson, J.; Pettersson, G. *Eur. J. Biochem.* **1978**, *87*, 1–8.
(16) Dooley, D. M.; McGuirl, M. A.; Mix, P. A. In *Biological and Inorganic Copper Chemistry*; Karlin, K. D., Zubieta, J., Eds.; Adenine Press: Guilderland, NY, 1986; pp 97–103.
(17) (a) Mims, W. B.; Peisach, J. In *Biological Magnetic Resonance*; Berliner, L. J., Reuben, J., Eds.; Plenum Press: New York, 1981; Vol. 3, pp 213–263. (b) Mims, W. B.; Peisach, J. In *Biological Applications of Magnetic Resonance*; Shulman, R. G., Ed.; Academic Press: New York, 1979; pp 221–269.
(18) (a) Mims, W. B.; Peisach, J. *Biochemistry* **1976**, *15*, 3863–3869. (b) Mondovi, B.; Graziani, M. T.; Mims, W. B.; Oltzik, R.; Peisach, J. *Biochemistry* **1977**, *16*, 4198–4202. (c) Peisach, J.; Mims, W. B.; Davis, J. L. *J. Biol. Chem.* **1979**, *254*, 4321–4323. (d) Zweier, J.; Aisen, P.; Peisach, J.; Mims, W. B. *J. Biol. Chem.* **1979**, *254*, 3512–3515. (e) Zweier, J. L.; Peisach, J.; Mims, W. B. *J. Biol. Chem.* **1982**, *257*, 10314–10316. (f) Fee, J. A.; Peisach, J.; Mims, W. B. *J. Biol. Chem.* **1981**, *256*, 1910–1914.
(19) Groh, S. E.; Nagahisa, A.; Tan, S. L.; Orme-Johnson, W. H. *J. Am. Chem. Soc.* **1983**, *105*, 7445–7446.
(20) (a) Mims, W. B.; Davis, J. L.; Peisach, J. *Biophys. J.* **1984**, *45*, 755–766. (b) Peisach, J.; Mims, W. B.; Davis, J. L. *J. Biol. Chem.* **1984**, *259*, 2704–2706.
(21) Mims, W. B. *Rev. Sci. Instrum.* **1974**, *45*, 1583–1591.
(22) Lin, C. P.; Bowman, M. K.; Norris, J. R. *J. Magn. Reson.* **1985**, *65*, 369–374.
(23) Britt, R. D.; Klein, M. P. *J. Magn. Reson.*, in press.
(24) Hahn, E. L. *Phys. Rev.* **1950**, *80*, 580–594.

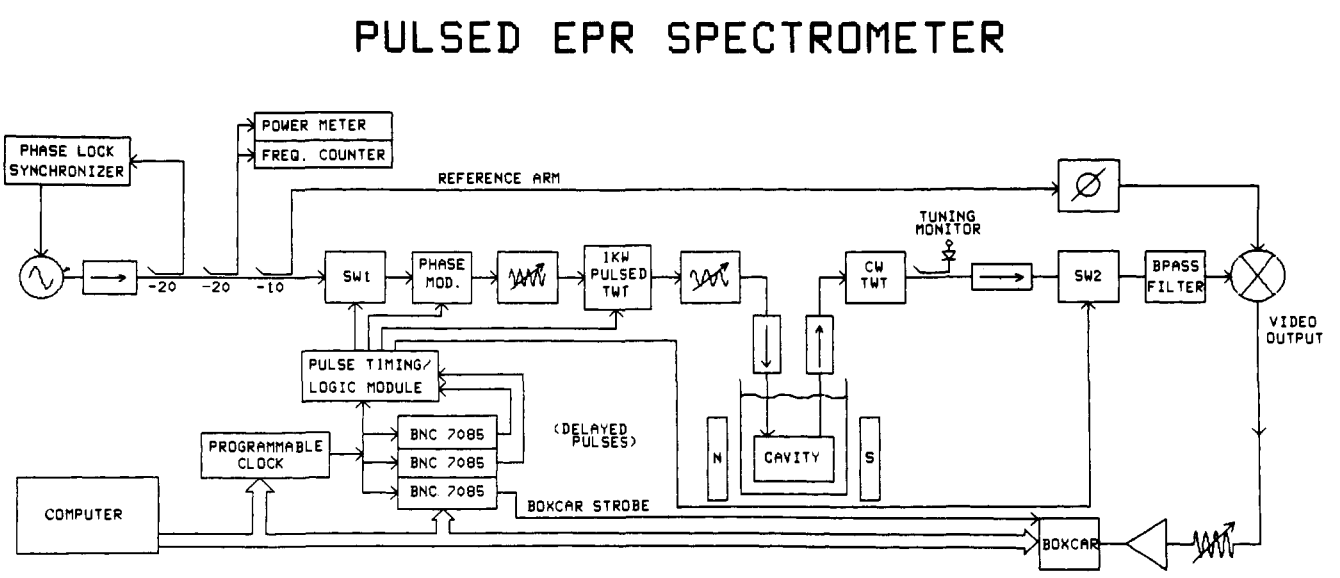

Figure 2. Block diagram of the pulsed EPR spectrometer used in these studies.

For studies where it was desirable to distinguish the contribution of ^2H in D_2O-exchanged samples from the contribution of ^{14}N and nonexchangeable protons, a data ratioing technique was used.[20a,b] This procedure involved collecting echo envelopes for two samples which differed only in that one was in aqueous buffer and the other in D_2O buffer. The data obtained from these samples were then normalized for signal intensity, and the ESE envelope obtained for the D_2O sample was divided by the envelope for the H_2O sample. Because the ESE envelope consists of the product of the modulation functions for all magnetically coupled nuclei multiplied by a decay function,[25a,b] this procedure yields a modulation pattern dominated by the deuterium superhyperfine interaction. (A more detailed discussion of the procedure and its applicability to frozen solution samples has been given by Mims et al.[20a]) Fourier transformation of ESE envelopes was carried out by using a modified version of the dead time reconstruction technique described by Mims.[26]

Copper(II)-mono-, -bis-, and -trisbipyridyl complexes were prepared according to the procedures given by Walker et al.[27] In each case, aliquots of 2,2'-bipyridyl dissolved in aqueous acetone (or D_2O/acetone, 10% acetone) were mixed with aqueous (or D_2O) solutions containing 5.0 mM $Cu^{II}(acetate)_2$. The pH of the resulting solution was then adjusted to 6.5, and the samples were diluted twofold by the addition of ethylene glycol. The final Cu(II) concentration for all samples was 2.5 mM, and the bipyridyl concentrations were 2.5 mM for the monobipyridyl complex, 5.0 mM for the bisbipyridyl adduct, and 25.0 mM for the trisbipyridyl complex.

Although both mono- and trisbipyridyl complexes are known to have tetragonally distorted octahedral geometry in solution,[27] the geometry and even the existence of the $Cu^{II}(bipy)_2$ species in solution has been questioned. X-ray crystallographic data obtained for $Cu^{II}(bipy)_2NO_2^-$[28] show that the Cu is in a cis distorted octahedral environment with the longer bonds being those between Cu and the chelating NO_2^- oxygens. Another X-ray study, performed on $Cu^{II}(bipy)_2(ClO_4)_2$, shows that this complex is a tetragonally distorted octahedron with the perchlorate ligands trans to one another and with a Cu-O bond length much greater than the Cu-N bond length.[29] Noack et al.,[30] using NMR and EPR techniques, concluded that $Cu^{II}(bipy)_2$ in solution at ambient temperatures is hexaccordinate, with the two water ligands cis to one another. At 77 K, EPR measurements indicate the presence of two species, and it was concluded that a cis-trans isomerization occurs upon lowering the temperature so that there are roughly equal populations of the two isomers under these conditions. Walker et al.[31] questioned this assignment and suggested that the two different EPR species seen were the consequence of $Cu^{II}(bipy)_2$ disproportionation to form $Cu^{II}(bipy)$ and $Cu^{II}(bipy)_3$. Our ESEEM results (see below) show that no tightly bound or "equatorial" waters are bound to $Cu(bipy)_2$ at 4.2 K. We conclude that the proposed disproportionation reaction does not occur.

In light of these results and the EPR parameters determined for $Cu^{II}(bipy)_2$ in frozen solution,[32] the bound water ligands can be considered axial as long as the axial direction is defined for those ligands that are bound at a longer distance from the Cu(II) than the four others. Finally, the possibility that $Cu^{II}(bipy)_2$ forms a five-coordinate, trigonal-bipyramidal complex in solution can be dismissed based on the EPR results which show $g_\parallel > g_\perp$.[33]

Bovine plasma amine oxidase (BPAO) was purified by modifications of literature procedures,[34] to be published elsewhere. Pig kidney amine oxidase (PKAO) was purified as previously described.[14b] All preparations used in these experiments were homogenous as judged by gradient and SDS gel electrophoresis and displayed specific activities and spectral properties consistent with high purity. Samples for pulsed EPR studies were extensively dialyzed against metal-free, 5.0 mM PIPES buffer, pH 7.0, containing 0.2 M NaCl and 2.0 mM EDTA. This was followed by dialysis against metal-free buffer, in order to remove the EDTA and salt, and then concentration by ultrafiltration to approximately 0.5 mM protein (1 mM Cu) in a stirred Amicon pressure cell with a YM-30 membrane. Samples were exchanged against deuteriated buffer by concentrating to a small volume in the stirred cell, then diluting with 5-10 volumes of deuteriated buffer, and repeating this several times over a period of 2-3 h. Cyanide and azide solutions were freshly prepared in buffer or distilled, deionized water prior to each series of experiments. Concentrations were such that negligible dilution of the protein solutions occurred upon anion addition.

Results and Discussion

I. Coordination of H_2O. A. H_2O Binding in Models. In order to provide a quantitative basis for the differentiation of water populations at or near the copper in amine oxidases, the ESE envelopes of copper(II)-mono-, -bis-, and -trisbipyridyl model compounds were studied in both H_2O and D_2O. These models were chosen because they allow one to separate ESE contributions from equatorially bound, axially bound, and ambient D_2O using the ratio method.[20b]

In all of the three model compounds studied, the magnetic coupling between equatorial ^{14}N is so large that its contribution to the echo envelope cannot be seen,[35] while contributions from axial ^{14}N are extremely weak and only provide a shallow perturbation on the data. In the simplest case, $Cu^{II}(bipy)_3$ in D_2O, the only deuterium significantly contributing to the envelope modulation is from ambient water as all of the primary coordi-

(25) (a) Rowan, L. G.; Hahn, E. L.; Mims, W. B. *Phys. Rev.* **1965**, *137*, A61-A71. (b) Mims, W. B. *Phys. Rev.* **1972**, *B5*, 2409-2419.
(26) Mims, W. B. *J. Magn. Reson.* **1984**, *59*, 291-306.
(27) Walker, F. A.; Sigel, H.; McCormick, D. B. *Inorg. Chem.* **1972**, *11*, 2756-2763.
(28) Procter, I. M.; Stephens, F. S. *J. Chem. Soc. A* **1969**, 1248-1255.
(29) Nakai, H. *Bull. Chem. Soc. Jpn.* **1971**, *44*, 2412-2415.
(30) Noack, M.; Gordon, G. *J. Chem. Phys.* **1968**, *48*, 2689-2699.
(31) Walker, F. A.; Sigel, H. *Inorg. Chem.* **1972**, *11*, 1162-1164.
(32) Peisach, J.; Blumberg, W. E. *Arch. Biochem. Biophys.* **1974**, *165*, 691-708.
(33) Elliot, H.; Hathaway, B. J.; Slade, R. C. *J. Chem. Soc. A* **1966**, 1443-1445.
(34) Turini, P.; Sabatini, S.; Befani, O.; Chimenti, F.; Casanova, C.; Riccio, P. L.; Mondovi, B. *Anal. Biochem.* **1982**, *125*, 294-298. Summers, M. C.; Markovic, R.; Klinman, J. P. *Biochemistry* **1979**, *18*, 1969-1979.
(35) Mims, W. B.; Peisach, J. *J. Chem. Phys.* **1978**, *69*, 4921-4930.

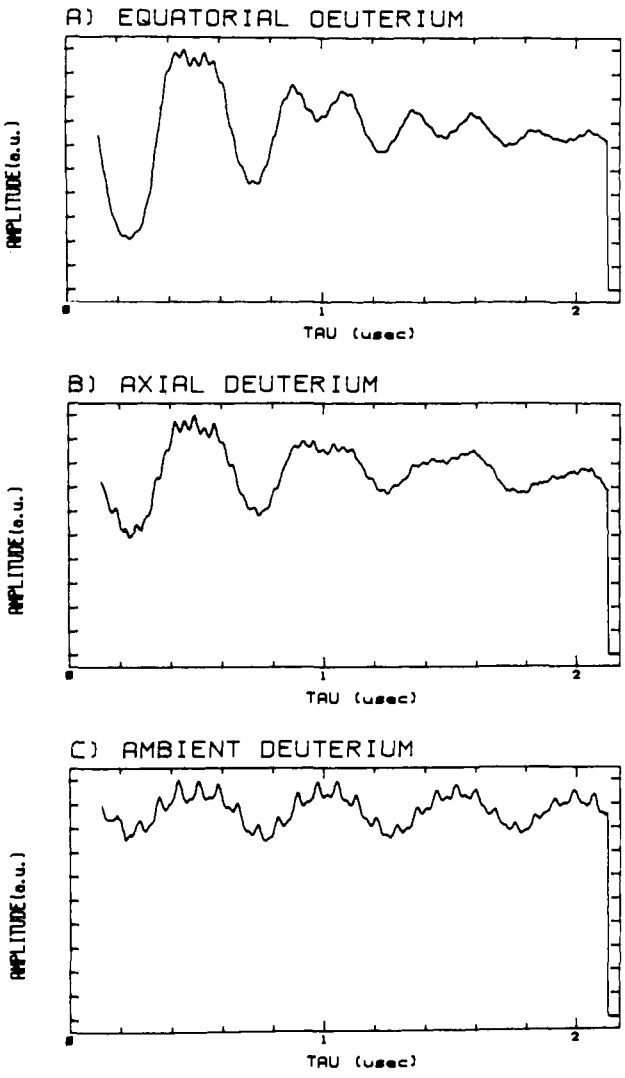

Figure 3. Two pulse electron spin echo envelope modulation (ESEEM) ratios for copper–bipyridyl model compounds. The traces are as follows: (a) The ESEEM pattern for equatorially bound D_2O was obtained by dividing the ratio of envelope modulations for Cu^{II}bipy in D_2O and in H_2O by the ratio of envelopes for $Cu^{II}(bipy)_2$ in D_2O and in H_2O. (b) The ESEEM pattern for axially bound D_2O was obtained by dividing the ratio of envelope modulation for $Cu^{II}(bipy)_2$ in D_2O and in H_2O by the ratio of envelopes for $Cu^{II}(bipy)_3$ in D_2O and in H_2O. (c) The ESEEM pattern for ambient D_2O was obtained by dividing the modulation envelope for $Cu^{II}(bipy)_3$ in D_2O by that for the same complex in H_2O. Conditions for the measurements were the following: microwave frequency, 8.7 GHz; microwave power, 50 W; magnetic field strength, 3000 G; and sample temperature, 4.2 K.

nation sphere sites of the Cu(II) are coordinated to the three bidentate ligands. However, nonexchangeable protons on the ligand as well as the axial ^{14}N atoms also contribute to the ESE envelope. In order to remove their contributions, the echo envelopes for the tris ligand complex in D_2O and H_2O were ratioed. The result is shown in Figure 3c.

For the $Cu^{II}(bipy)_2$ complex in D_2O where equatorial ligand positions are occupied by ligand ^{14}N, there are two populations of interacting deuterons: the more strongly coupled from axial water ligands to Cu(II) and the remainder from ambient water. By taking the ratio of the ESE obtained under identical conditions for the bis complex in D_2O and the same complex in H_2O, the contribution of both populations of deuterons is obtained, and the modulation arising from nonexchangeable protons is largely cancelled. By further dividing this result with that obtained from the above for ambient D_2O interactions observed for the $Cu^{II}(bipy)_3$ complex, one obtains the ESE contribution from deuterium on axially coordinated D_2O (Figure 3b). Similarly, by dividing the ESE decay envelope ratio for the Cu^{II}bipy complex obtained in D_2O and in H_2O by the analogous ratio for the $Cu^{II}(bipy)_2$ complex, one obtains the envelope modulation for equatorially bound D_2O (Figure 3a).

Examination of Figure 3 shows that for inner coordination sphere D_2O, that which is bound equatorially and axially (Figure 3 (parts a and b)), ESE envelope modulations with periods of approximately 500 and 250 ns are observed. These modulations, at approximately 2 and 4 MHz, correspond to the first and second harmonics of the deuterium nuclear Zeeman frequency at 3 kG. For equatorially bound D_2O (Figure 3a), the deuteron modulation is deep; there is a large second harmonic contribution to the ESE pattern, and the first harmonic is heavily damped. For axially bound D_2O (Figure 3b), the modulation is less deep, the second harmonic contribution to the ESE pattern is less pronounced, and the damping of the first harmonic is not as severe as it is in the equatorial case. These trends are continued for ambient D_2O (Figure 3c) and are in agreement with the theoretical predictions of Mims et al.[36] and Kevan.[37]

B. H_2O Binding in Proteins. To examine the possibility of H_2O ligation to the Cu(II) in amine oxidases, each sample was studied in aqueous and in D_2O-exchanged media. The two pulse ESE modulation envelope obtained for the D_2O-exchanged sample was then divided by that obtained for the sample in aqueous buffer, and an ESE envelope primarily due to exchangeable deuterons magnetically coupled to Cu(II) was obtained, in a way analogous to that for the model compounds. The result of this procedure for porcine kidney amine oxidase, PKAO, is shown in Figure 4a and is similar to that seen in a study of the bovine plasma enzyme. The deuterium modulation is fairly deep, as compared with that obtained for copper proteins such as azurin where the metal is shielded from water by endogenous, nonaqueous ligands[20a] and resembles that obtained for the Cu^{II}bipy models where water is in the primary coordination sphere of the metal ion. It is for this reason that we suggest that the observed deuterium modulation for amine oxidase is due to both inner- and outer-sphere-coordinated deuterons.

The ratio of ESE envelopes for the cyanide derivative of PKAO studied in D_2O and in H_2O differs markedly from that of the native enzyme and is shown in Figure 4b. The deuterium modulation depth has decreased about twofold, and little or no second harmonic near 4 MHz can be seen.

The ESE modulation pattern for the deuterium displaced by cyanide can be obtained by dividing the data of Figure 4a, that arising from deuterium interacting with Cu(II) in the native protein, by the data of Figure 4b, that arising from exchangeable deuterons in the cyanide derivatized protein, and is displayed in Figure 4c. Although the early portion of the trace in Figure 4c is somewhat distorted due to the presence of deep ^{14}N modulation in the raw data, deep modulation at both the first and second harmonic of the deuterium nuclear Zeeman frequency is observed. Further, the ESE pattern of Figure 4c is indicative of inner sphere, or closely coordinated deuterium[36,37] (see below) resembling that shown in Figure 3a and is consistent with the view that CN^- addition has caused displacement of inner coordination sphere D_2O from the Cu(II) site.

Similar results were obtained for the bovine plasma amine oxidase by using azide rather than cyanide as the anion bound to the protein (Figure 5).

C. Simulation of Echo Envelopes for Deuterium. A detailed analysis of the data for the various copper^{II}–bipyridyl complexes presented in Figure 3 was achieved by envelope simulation with use of the density matrix formalism for simulating ESE envelopes developed by Mims.[25b] The general expression for a two pulse envelope modulation function is given by

$$E_{mod}(\tau) = (2I + 1)^{-1} \mathrm{Tr}\{\mathbf{Q}_\tau^\dagger \mathbf{M}^\dagger \mathbf{P}_\tau^\dagger \mathbf{M} \mathbf{Q}_\tau \mathbf{M}^\dagger \mathbf{P}_\tau \mathbf{M}\} \quad (4)$$

where **Q**, **P**, and **M** are matrices of dimension $2I + 1$. P and Q

(36) Mims, W. B.; Peisach, J.; Davis, J. L. *J. Chem. Phys.* **1977**, *66*, 5536–5550.

(37) Kevan, L. In *Time Domain Electron Spin Resonance*; Kevan, L., Schwartz, R. N., Eds.; Wiley-Interscience: New York, 1979; pp 279–342.

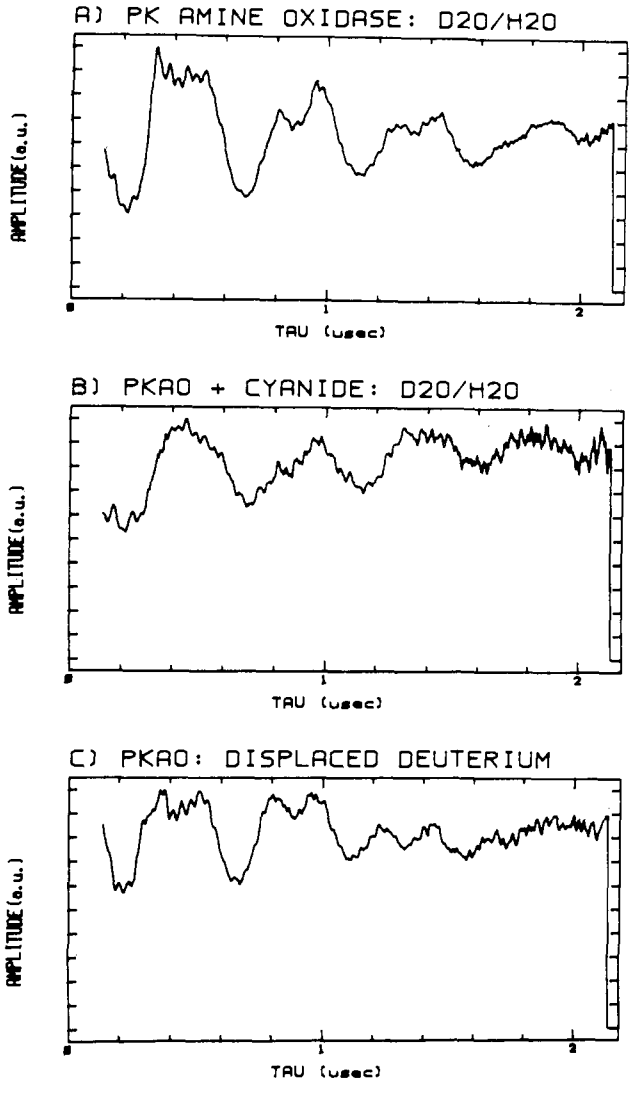

Figure 4. Ratios of two pulse ESEEM data for porcine kidney amine oxidase, PKAO, and its cyanide derivative. The ratios were obtained by using the following data sets: (a) PKAO in D_2O-exchanged buffer/PKAO in aqueous buffer; (b) PKAO + CN^- in D_2O-exchanged buffer/PKAO + CN^- in aqueous buffer; and (c) trace a/trace b. Data were collected under the following conditions: microwave frequency, 9.5 GHz; microwave pulse power, 30 W; microwave pulse duration, 20 ns; magnetic field strength, 3300 G; and sample temperature, 4.2 K.

are submatrices of the rotation operator that describes the time evolution of the density matrix during the free-precession periods for the two-electron spin manifolds. The modulation depths of the frequency components contained in **P** and **Q** are given by the elements of **M**, where

$$\mathbf{M} = \mathbf{M}_\alpha^\dagger \mathbf{M}_\beta \tag{5}$$

$\mathbf{M}_\alpha$ and $\mathbf{M}_\beta$ are matrices which diagonalize the spin Hamiltonian that describes the superhyperfine splittings in the $|\alpha\rangle$ and $|\beta\rangle$ electron spin manifolds, respectively.

The Hamiltonian used to model the superhyperfine splittings for the deuterium modulation data presented above consists of terms describing the nuclear Zeeman, electron-nuclear hyperfine, and nuclear quadrupole interactions and is given by

$$\mathcal{H}_N = \mathcal{H}_{\text{nucl Zeeman}} + \mathcal{H}_{\text{hf}} + \mathcal{H}_Q \tag{6}$$

where

$$\mathcal{H}_{\text{nucl Zeeman}} + \mathcal{H}_{\text{hf}} = \sum_{i=x,y,z} (m_s A_{ii} - \nu_n) l_i \hat{I}_i \tag{7}$$

and

$$\mathcal{H}_Q = \tfrac{1}{4} e^2 q Q [(3\hat{I}_z'^2 - 2) + \eta(\hat{I}_x'^2 - \hat{I}_y'^2)] \tag{8}$$

The above expressions assume **g** tensor isotropy and that the

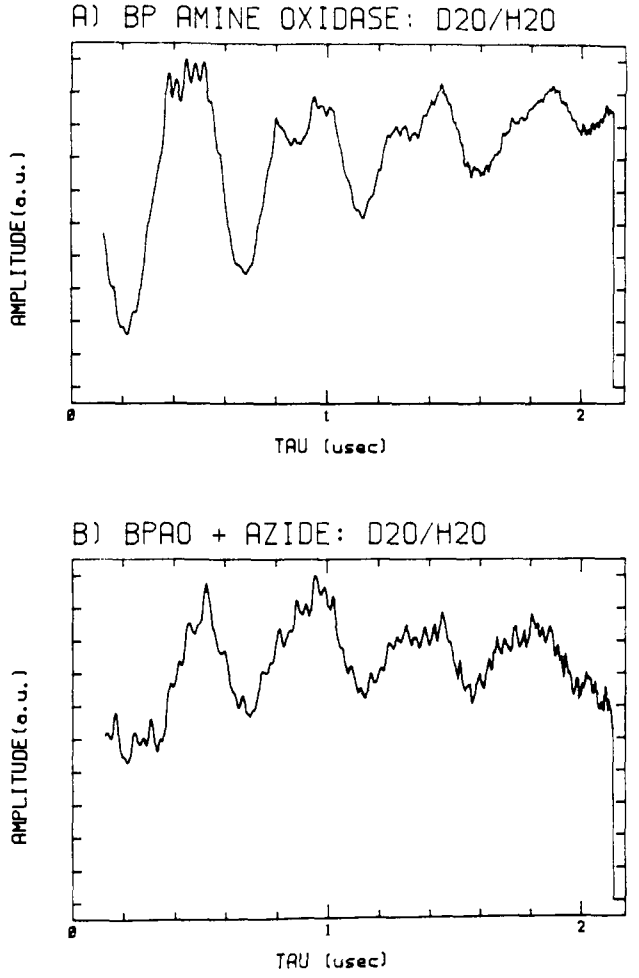

Figure 5. Ratio of ESE envelope modulations obtained as in Figure 4 but for (a) bovine plasma amine oxidase, BPAO, and (b) BPAO + N_3^-. Experimental conditions were identical with those given for Figure 4.

Hamiltonian is to be evaluated in the principal axis system (PAS) of the hyperfine coupling tensor. The terms A_{ii} in eq 7 are the elements of the hyperfine tensor, ν_n is the nuclear Zeeman frequency, and l_i terms are direction cosines relating the direction of the applied static magnetic field to the PAS of the hyperfine tensor, and the $\hat{I}_i$ are the nuclear spin operators. The nuclear quadrupole interaction (nqi) is described by the Hamiltonian given in eq 8. The five parameters needed to model the nqi are as follows: e^2qQ, the quadrupole coupling constant; η, the asymmetry parameter; and the three Euler angles α, β, and γ, which describe the relationship between the principal axis systems of the hyperfine and nqi tensors. The nuclear spin operators of eq 8 are primed because they refer to the nqi PAS, while those of eq 7 refer to the hyperfine tensor PAS.

In an ESE calculation, the Euler angle rotation of the nqi spin operator is done first, and then this "effective" set of parameters is used along with the rest of $\mathcal{H}_N$ to calculate the Hamiltonian matrix for both electron spin sublevels. The two matrices are then diagonalized, and the eigenvalues are used to compute the elements of **P** and **Q**, while the eigenvectors are used to set the elements of **M**. The results are then used in eq 4, and the modulation function for a given set of direction cosines, l_i, is computed. This procedure, except for the Euler angle rotation, is then repeated for all possible orientations of $\mathcal{H}_0$ with respect to the principal axis system of the hyperfine coupling tensor in order to obtain a powder average modulation function.

The input parameters for a calculation are as follows: g_n, the nuclear g value; A_{xx}, A_{yy}, and A_{zz}, the elements of the hyperfine tensor; $\mathcal{H}_0$, the magnetic field strength used in the measurement; and the five nuclear quadrupole interaction parameters, e^2qQ, η, α, β, and γ. For the simulation of electron spin echo envelope modulation (ESEEM) data arising from axially and equatorially

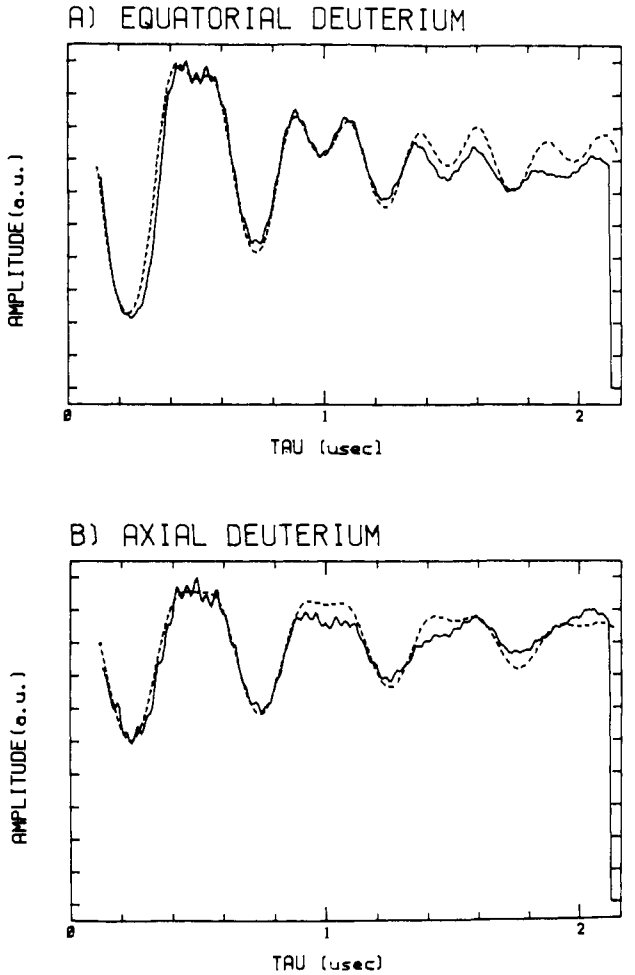

Figure 6. Comparison of experimental ESEEM data (solid lines) with simulated data (dashed lines) for (a) equatorially bound D_2O and (b) axially bound D_2O. The experimental results as in Figure 4 are derived from studies of copper(II)–bipyridyl model compounds in D_2O and H_2O. Parameters common to both simulations were as follows: e^2qQ, 0.22 MHz; η, 0.1; β, 17°; magnetic field strength, 3000 G; g_n, 0.85741; and three deuterons at an equal distance were considered. Parameters that differ between the two simulations were for (a) equatorially bound D_2O, $A_{xx} = A_{yy} = -0.37$ MHz, $A_{zz} = 1.34$ MHz ($a = 0.2$ MHz, $r = 2.8$ Å), and for (b) axially bound D_2O, $A_{xx} = A_{yy} = -0.25$ MHz, $A_{zz} = 0.80$ MHz ($a = 0.1$ MHz, $r = 3.3$ Å).

bound D_2O molecules in the various copper–bipyridyl complexes, the hyperfine tensor was taken to be axial with tensor elements

$$A_{xx} = A_{yy} = a - F$$

$$A_{zz} = a + 2F \quad (9)$$

where a represents the Fermi contact interaction and in terms of the point dipole–dipole model

$$F = g_e g_n \beta_e \beta_n / r^3 \quad (10)$$

The term g_e in eq 10 is the experimental electron g value, and r is the effective distance between the unpaired electron and the magnetically coupled nucleus. For the nqi parameters, the e^2qQ and η values used in the calculations were those determined by NQR measurements on deuteriated Ice II.[38] The principal axis of the nqi tensor in D_2O is expected to be along the O–D bond, while the principal axis of the hyperfine coupling tensor probably lies somewhere between the vector defined by the O–D bond and that defined by a line connecting the Cu(II) and the deuteron being considered. Because both tensors involved are nearly axial, the

(38) Edmonds, D. T.; Goren, S. P.; Mackay, A. L.; White, A. A. L.; Sherman, W. F. *J. Magn. Reson.* **1976**, *23*, 505–514.

Table I. Equatorial and Axially Bound D_2O Parameter Sets[a]

equatorial	axial
$r = 2.8$ Å (±0.1 Å)	$r = 3.3$ Å (±0.1 Å)
$a = 0.2$ MHz (±0.1 MHz)	$a = 0.1$ MHz (±0.1 MHz)
$e^2qQ = 0.22$ MHz	$e^2qQ = 0.22$ MHz
$\eta = 0.1$	$\eta = 0.1$
$\beta = 17°$ (±10°)	$\beta = 17°$ (±10°)
$\mathcal{H} = 3000$ G	$\mathcal{H} = 3000$ G
3 deuterons	3 deuterons

[a] Hamiltonian parameters used for ESE envelope simulation shown in Figure 6.

Euler angles α and γ were fixed at 0°, and the angle β was varied from 0 to 40°. Therefore, in the calculations only three parameters were varied in an attempt to account for the copper–bipyridyl ESEEM data: a, the Fermi contact term; r, the effective dipole–dipole distance; and β, the angle between the principal axis of the hyperfine and nqi tensors.

ESEEM simulations for the copper–bipyridyl data displayed in Figure 3 (parts a and b, dashed lines) are shown in Figure 6 along with the experimental data (solid line). Because all of the model compounds were prepared in 50% v/v D_2O/ethylene glycol ($Et(OH)_2$) and there is rapid exchange between the deuterons on D_2O and the glycol alcoholic protons, there is a significant amount of HDO and H_2O in solution. According to the equilibrium expression for this exchange

$$2D_2O + 2Et(OH)_2 \rightleftarrows HDO + H_2O + Et(OD)_2 + Et(OD)(OH) \quad (11)$$

the various model compound solutions contained approximately 19.3 M D_2O, 4.1 M HDO, and H_2O. Therefore, the two equatorial waters or the two axial waters that give rise to the modulation data of Figure 3 (parts a and b) will not consist entirely of D_2O. For every two molecules of water coordinated to a Cu(II) there will be 1.4 molecules of D_2O, 0.3 molecule of HDO, and 0.3 molecule of H_2O. Thus, equatorial or axial water pairs that give rise to the modulation data in Figure 3 (parts a and b) will each contain approximately three deuterons. The simulation results displayed in Figure 6 were each obtained by cubing a modulation pattern due to one magnetically coupled deuterium assuming a spherical model for contribution to modulation.[39] The parameter sets for equatorial and axial water used in the simulations of Figure 6 are given in Table I.

The agreement between experimental results and a theoretical simulation of modulations shown in Figure 6 is fairly good. The distances obtained by using the point dipole–dipole approximation for copper and deuterium on coordinated water yield Cu^{II}–O bond distances of 2.1 and 2.6 Å for equatorially and axially bound D_2O, respectively. These numbers are in good agreement with those measured by Suryanarayana et al. for D_2O coordination to Cu(II) in polyvinyl alcohol matrices, 2.2 and 2.7 Å, respectively.[40] Any disagreement between experiment and theory for the copper–bipyridyl work presented here could arise from several factors. (i) The Cu(bipy) and $Cu(bipy)_2$ compounds were prepared with stoichiometric amounts of bipyridyl. Yet, according to Walker et al.,[27] these solutions will be only about 85% pure, with 6% each Cu^{II}aquo and $Cu^{II}(bipy)_2$ contaminants in the $Cu^{II}(bipy)$ sample and about 7% each $Cu^{II}(bipy)$ and $Cu^{II}(bipy)_3$ in the $Cu^{II}(bipy)_2$ sample. (ii) No attempt was made to correct for difference in envelope decay functions for samples in H_2O and in D_2O. It was assumed that the ratio process would remove this component from the data for a two pulse measurement. (iii) Several approximations were made in the calculations, the most serious being use of the spherical model[39] and the assumption of an isotropic **g** tensor.

An attempt was also made to use the Hamiltonian parameters for equatorially bound D_2O, as given in Table I, to simulate the modulation pattern due to the displacement of D_2O upon cyanide

(39) Kevan, L.; Bowman, M. K.; Narayana, P. A.; Boeckman, R. K.; Yudanov, V. F.; Tsvetkov, L. *J. Chem. Phys.* **1975**, *63*, 409–416.
(40) Suryanarayana, D.; Narayana, P. A.; Kevan, L. *Inorg. Chem.* **1983**, *22*, 474–478.

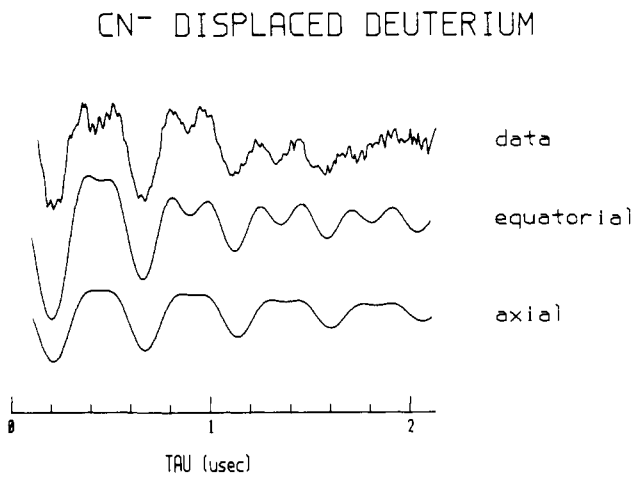

Figure 7. Comparison of the experimental two pulse ESEEM data (upper trace) obtained for the cyanide displaced deuterium in porcine kidney amine oxidase (Figure 4c) and theoretical predictions using the Hamiltonian parameters obtained for the equatorially bound D_2O (center trace) and axially bound D_2O (bottom trace) in copper(II)-bipyridyl complexes. The parameters used in the calculation were identical with those of Figure 6 except for the magnetic field strength, 3300 G, and number of equivalent deuterons, two. The ESEEM patterns are plotted on identical scales but are arbitrarily offset from one another.

binding to PKAO (Figure 4c). The only calculation parameter that is different from those in Table I is the magnetic field strength, which was changed to correspond to the experimental value, and the number of deuterons, which was changed to two (corresponding to one D_2O molecule displaced). The simulation (Figure 7) corresponding to the displacement of an equatorially bound D_2O molecule clearly accounts for the relative amplitudes and damping of the deuterium first and second harmonic frequency components better than the simulation corresponding to the displacement of an axially bound D_2O. However, the agreement between experiment and simulation for the enzyme data is less good than for the model compounds. This is due, in part, to the reasons given above but also due to distortions in the ratio data that arise because of deep ^{14}N modulation present in the raw ESEEM data.

In addition, the ligand geometry about the Cu(II) center in the native protein is known to be somewhat irregular, as evidenced from the rhombic EPR spectrum.[11a] Nevertheless, the results of Figure 7 clearly show that the addition of cyanide to porcine kidney amine oxidase has caused the loss of a tightly bound D_2O molecule with ESEEM properties similar to those found for equatorially bound D_2O in the Cu^{II}(bipy) model compound. Similar studies with azide added to bovine plasma amine oxidase (Figure 5) have been analyzed in the same way and also lead to the conclusion that tightly bound D_2O is displaced when the anion is bound.

A comparison of the deuterium modulation patterns for cyanide-treated porcine kidney protein (Figure 4b) and azide-treated bovine protein (Figure 5b) with the modulation patterns for axially bound and ambient D_2O, as derived from model compound studies (Figure 3 (parts b and c)), suggests that the concentration of interacting deuterons is greater in the anion treated proteins than can be accounted for by ambient water deuterons alone. As it is likely that the Cu(II) bound to the protein interacts with less ambient deuterons than does Cu(II) in the trisbipyridyl model, it is suggested that a water molecule remains bound axially to the Cu(II) in the protein when cyanide or azide is also bound. However, no definite conclusions concerning other possible bound waters can be drawn, because it is difficult to differentiate the contributions of ambient water from those for exchangeable protons on the protein molecule.

II. Nitrogen Coupling. ESE envelope modulations due to ^{14}N magnetically coupled to the Cu(II) site were studied by using the stimulated echo technique.[24] A Fourier transform of the modulation data obtained for pig kidney amine oxidase is shown in Figure 8a. The frequencies arise from bound imidazole in at least two magnetically distinct environments. This interpretation is

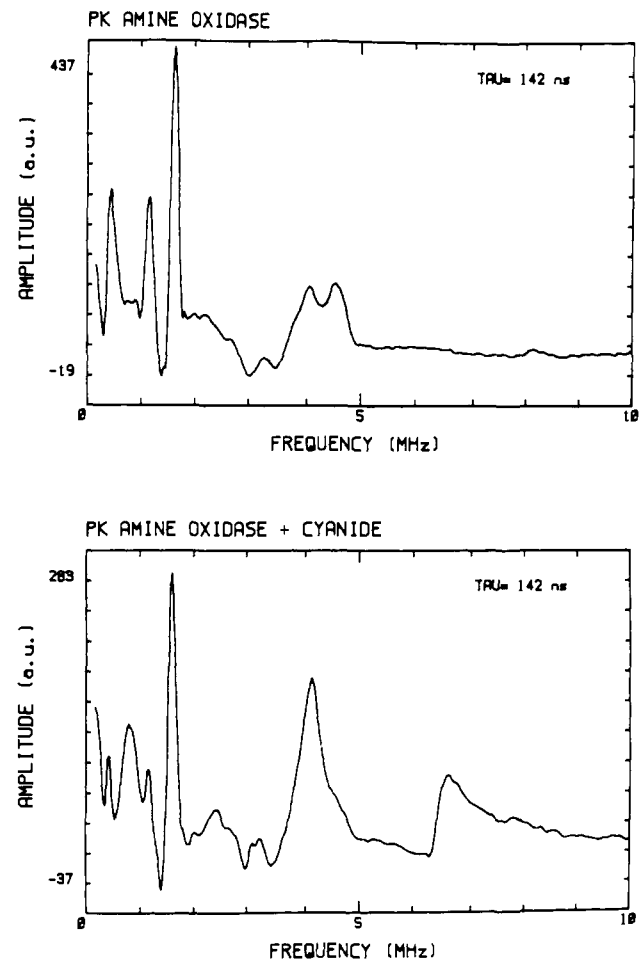

Figure 8. Cosine Fourier transforms of stimulated echo data obtained for (a) native porcine kidney amine oxidase and (b) the same protein + CN^-. The conditions for these measurements were as follows: microwave frequency, 9.5 GHz; microwave power, 20 W; magnetic field strength, 3300 G; τ, 142 ns; and sample temperature, 4.2 K.

based on ESEEM studies of Cu^{II}(diethylenetriamine)(imid) and $Cu^{II}(imid)_4$ by Mims and Peisach.[35] These authors demonstrated that ESE envelope modulations were due to coupling to the remote nitrogen of bound imidazole, the coupling from directly coordinated ^{14}N being too large and outside the range for ESE spectroscopy. The data can be analyzed by using the following Hamiltonian parameters: a, the Fermi contact term, 1.75 MHz; r_{eff} = 2.9 Å; and the nuclear quadrupole parameters, e^2qQ = 1.43 MHz, η = 0.9. Because $a/2$ is approximately equal to the nuclear Zeeman frequency at 3 kG, the magnetic field used for these studies, the energy level splittings of one of the electron spin manifolds is almost completely determined by the ^{14}N nuclear quadrupole interaction. As a result, the hyperfine splittings are nearly independent of orientation, and one should observe three sharp lines in the Fourier transform of the ESEEM data from this manifold. For both model compounds, the zero-field nuclear quadrupole resonance data for histidine imidazole[41] predicts that the components from this spin manifold will appear at 0.65, 0.75, and 1.40 MHz. Mims and Peisach observed two low-frequency components for their models, a narrow line at 1.4 MHz and a wider line at 0.7 MHz, presumably made up of narrow 0.65- and 0.75-MHz components.

The second electron spin manifold, where nuclear hyperfine and nuclear Zeeman terms are additive, gives rise to much broader spectral lines. Normally, only the transition between the outermost levels is resolved. For Cu^{II}(det)(imid) and $Cu^{II}(imid)_4$ models studied near 3 kG, this transition occurs at 4.0 MHz (approximately $2\nu_N + a$).

(41) Edmonds, D. J.; Summers, C. P. *J. Magn. Reson.* **1973**, *12*, 134–142.

Table II. ^{14}N Coupling Parameters for Coordinated Imidazoles in Porcine Kidney Amine Oxidase

(1) "Normal Configuration" Peaks at 0.7, 1.4, 4.0 MHz
a = 1.8 MHz
effective e^2qQ = 1.43 MHz
effective η = 0.91
(2) "Strong-Coupled" Peaks at 0.45, 1.1, 1.55, 4.5 MHz
a = 2.3 MHz
effective e^2qQ = 1.7 MHz
effective η = 0.5

[a] Hamiltonian parameters derived from analysis of the ^{14}N frequency data for porcine kidney amine oxidase shown in Figure 8.

For pig kidney amine oxidase studied at 3 kG, one observes sharp resonance lines at 0.45, 1.1, and 1.6 MHz (Figure 8a). In addition, there is a slightly broader line at 0.7 MHz and two broad components at 4.0 and 4.5 MHz. The data for native bovine plasma amine oxidase (Figure 9a) are similar to those for the porcine kidney enzyme, except that the spectral components around 4 MHz are not as well resolved. However, the width of this component is similar to that of the porcine protein and is taken as an indication of frequency components at 4.0 and 4.5 MHz. To account for these six spectral features one needs to invoke a model consisting of two types of magnetically independent, coordinated imidazoles. Their magnetic environments differ in that both the Fermi contact interaction and the effective nuclear quadrupole coupling parameters are different. A preliminary analysis yields the two sets of coupling constants given in Table II. Three points should be made concerning this analysis. (a) One type of imidazole, the more strongly coupled, has a contact interaction, 2.3 MHz, that is 0.5 MHz higher than that found for the other, more weakly coupled imidazole in porcine kidney amine oxidase. The weaker one resembles that in Cu^{II}(imid) model compounds. (b) The effective nuclear quadrupole parameters[42] are also different for the two types of imidazoles. While one has quadrupole parameters similar to those of Cu^{II}(imid) model complexes, the second has a higher e^2qQ and a much lower asymmetry parameter, η. (c) The anisotropy in the hyperfine coupling cannot be determined until full envelope simulations are carried out.

The addition of CN^- to the porcine protein alters the structure of the ligand environment of the Cu(II) in addition to displacing H_2O from the Cu(II) site (see above). The appearance of a peak at 6.6 MHz in the Fourier transform of three pulse data taken at short τ (Figure 8b) is indicative of $C^{14}N^-$ binding to Cu(II). This peak is also observed for the model Cu^{II}(dien)$C^{14}N^-$ and, due to the shallowness of its modulation, is probably the only ^{14}N component that will be observed by ESE methods for a Cu(II) complex that contains imidazole. This component is absent when $C^{15}N^-$ is added to the protein, even though the same changes still occur in the imidazole coupling as when $C^{14}N^-$ is bound (see below). Although only a preliminary analysis has been done on the Cu^{II}(dien)$C^{14}N^-$ complex, an ESEEM study of Cu^{II}-(dien)$C^{15}N^-$ indicates that the Fermi contact interaction for the cyanide–^{14}N coupled to Cu(II) is about 4.3 MHz.

The addition of $C^{14}N^-$ to porcine kidney amine oxidase causes a significant change in the imidazole coupling (Figure 8b). The data show a decrease in the relative intensity of the 0.4- and 1.1-MHz components and an increase in the 0.7-MHz component. Also, the 4.0- and 4.5-MHz components coalesce and give rise to a single peak at 4.1 MHz. Since there is little change in the overall modulation depth, the data probably reflect a change in the magnetic coupling of the "stronger coupled" imidazole found in the native protein to a magnetic environment similar to that found in Cu^{II}(imid) model complexes. It appears, therefore, that the binding of CN^- forces the imidazoles at the Cu(II) site into magnetically equivalent environments.

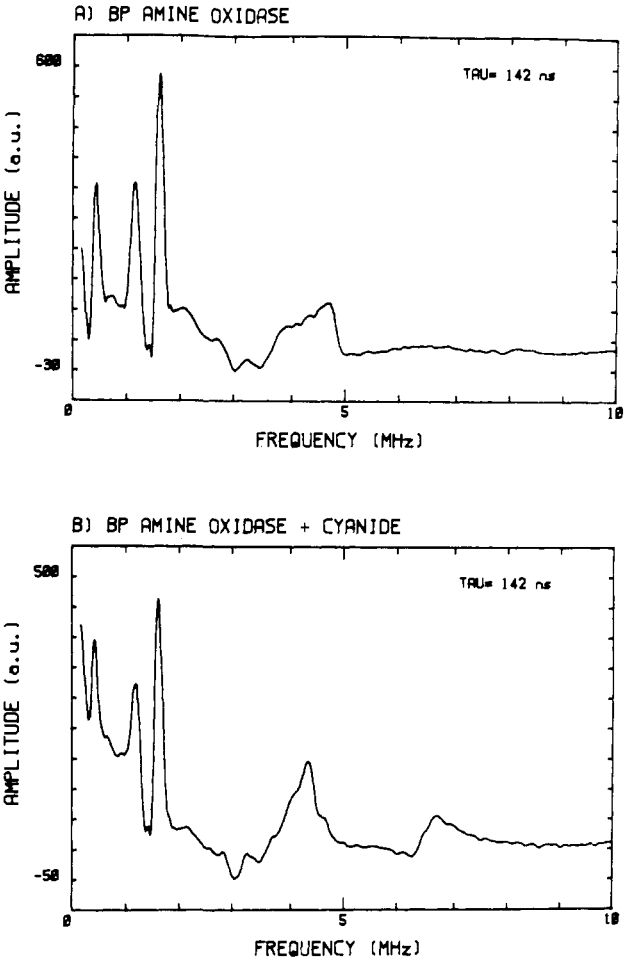

Figure 9. Cosine Fourier transforms of stimulated echo data obtained for (a) native bovine plasma amine oxidase and (b) the same protein + CN^-. The conditions for these measurements were identical with those given for Figure 8.

The addition of $C^{14}N^-$ to bovine plasma enzyme also gives rise to a spectral component at 6.6 MHz (Figure 9b), proving that CN^- binds to the Cu(II) in a magnetically similar fashion as in the porcine protein and in the Cu^{II}(dien)CN^- model. For bovine plasma amine oxidase the quadrupole lines at 0.4 and 1.1 MHz do not appear to change with the addition of either CN^- or N_3^-, but the components near 4 MHz appear to coalesce, as for porcine kidney oxidase, but to 4.3 MHz, indicating that imidazole is coupled differently to Cu(II) in this enzyme (the contact interaction is about 0.2 MHz greater) when anion inhibitors are bound.

III. Summary. The pulsed EPR results presented in this paper substantiate several aspects of the proposed model for the copper sites in amine oxidases shown in Figure 1. Specifically, the data establish that water is tightly bound to Cu(II) and this is displaced by cyanide or azide. Also there are different populations of imidazoles coordinating to Cu(II) in the native protein, in two magnetically inequivalent environments. Inhibitory anions displace equatorial water but probably leave an axial water molecule bound to Cu(II). Moreover, solvent ^1H NMR relaxation measurements are consistent with the view that water is bound to copper(II)–anion complexes in amine oxidases, likely axially coordinated, in rapid exchange with solvent water.[11b]

Previous ENDOR measurements on porcine plasma amine oxidase[12] suggest that azide displaces all bound water from Cu(II) or decreases the Cu^{II}–H_2O interactions such that they are no longer detectable. However, these conclusions are somewhat questionable considering the low signal-to-noise ratio for certain ENDOR spectra and the lack of a detailed analysis.

(42) The word "effective" is used here because knowledge of the relationship between the principal axis systems of the hyperfine tensor and nuclear quadrupole interaction tensor must be known before the true e^2qQ and η can be computed. It is possible that the large change in the effective η just reflects a change in the relative directions of the nqi and hyperfine principal axis systems and not a real change in the electric field gradient asymmetry about the remote nitrogen. However, in either case the higher e^2qQ is needed to predict the 1.55-MHz component.

Axial and equatorial H_2O molecules have also been proposed as ligands in dopamine-β-hydroxylase,[43] galactose oxidase,[44] and the type 2 copper sites in multicopper oxidases;[45] histidine imidazoles are known to be Cu(II) ligands in these enzymes as well.[43-45] Despite the apparent structural similarities in the metal binding sites in these various Cu(II) containing enzymes, there is nevertheless considerable variation in the chemical and physical properties of the copper sites and in their probable catalytic roles.[4,5,43-45] Copper ions in amine oxidases are not involved in substrate amine binding[5,9] but evidently are essential for the oxidation of the substrate reduced enzyme by O_2.[4-7,9,45,46] Since N_3^- and especially CN^- are effective amine oxidase inhibitors, the ESE modulation results presented here suggest that the labile coordination position on at least one copper ion is important for catalysis. Its role may be a direct one, e.g., as in the proposal that equatorially coordinated hydroxide nucleophilically assists hydride transfer from the reduced organic cofactor to O_2,[47] or some electronic or structural property of the copper site, which is crucial for enzyme turnover, may be sensitive to equatorial ligand substitution.

Acknowledgment. We thank W. E. Blumberg, D. Zuckerman, and W. B. Mims for advice and technical assistance concerning the design of the pulsed EPR spectrometer used in these measurements and the analysis of ESEEM data. We also thank Cheryl Cote and Michele McGuirl for their dedicated and excellent technical assistance. That portion of this research carried out at Albert Einstein College of Medicine is supported by United States Public Health Service Grants RR-02583 and HL-13399. That portion of this research carried out at Amherst College is supported by the United States Public Health Service Grant GM-27659.

(43) Hasnain, S. S.; Diakun, G. P.; Knowles, P. F.; Binsted, N.; Garner, C. D.; Blackburn, N. J. *Biochem. J.* **1984**, *221*, 545-548.
(44) Kosman, D. J. In *Copper Proteins and Copper Enzymes*; Lontie, R., Ed.; CRC Press: Boca Raton, FL, 1984; Vol. 2, pp 1-26, and references cited therein.
(45) (a) Reinhammar, B.; Malmstrom, B. G. In *Copper Proteins*; Spiro, T. G., Ed.; Wiley: New York, 1981; pp 109-149. (b) See, also: *Copper Proteins and Copper Enzymes*; Lontie, R., Ed.; CRC Press: Boca Raton, FL, 1984; Vol. 3, for several reviews on multicopper oxidases.
(46) (a) Suzuki, S.; Sakurai, T.; Nakahara, A.; Manabe, T.; Okuyama, T. *Biochemistry* **1983**, *22*, 1630-1635. (b) Bellelli, A.; Brunori, M.; Finazzi-Agro, A.; Floris, G.; Giartosi, A.; Rinaldi, A. *Biochem. J.* **1985**, *232*, 923-926.
(47) (a) Kelly, I. D.; Knowles, P. F.; Yadav, K. O. S.; Bardsley, W. G.; Leff, P.; Waight, R. D. *Eur. J. Biochem.* **1981**, *114*, 133-138. (b) Yadav, K. O. S.; Knowles, P. F. *Eur. J. Biochem.* **1981**, *114*, 139-144.

Molecular Spectroscopy of High-Spin Co(II). Polarized Single Crystal Electronic Absorption Spectra of Structurally Defined Tetracoordinate Complexes with Sulfur-Donor Ligands[1a]

Marvin W. Makinen,*[†1b] Susan C. Hill,[†] Michael Zeppezauer,[‡] Cindy L. Little,[†] and Jeremy K. Burdett[⊥]

Contribution from the Department of Biochemistry and Molecular Biology, The University of Chicago, Cummings Life Science Center, Chicago, Illinois 60637, Fachbereich Biologische Chemie 15.2, Universität des Saarlandes, D-6600 Saarbrücken, Federal Republic of Germany, and Department of Chemistry, The University of Chicago, Chicago, Illinois 60637.
Received May 9, 1986

Abstract: The polarized single crystal electronic absorption spectra of active site specific Co^{2+}-reconstituted horse liver alcohol dehydrogenase and of its binary inhibitor complexes formed with imidazole and pyrazole have been determined in the 42000-8000-cm^{-1} range. There are, in general, three characteristic clusters of bands: low-intensity bands ($f \simeq 0.001$) in the near-infrared near 10000 cm^{-1}, medium-intensity bands ($f \simeq 0.01$) in the 20000-15000-cm^{-1} region, and high-intensity bands ($f \simeq 0.1$) in the 30000-25000-cm^{-1} region. The spectra are assigned on the basis of the polarized single crystal spectrum of $Co[SC(CH_3)_2CH_2NH_2]_2$ and extended Hückel calculations of model complexes. The weak bands in the near-infrared region are assigned to ligand-field transitions of the high-spin Co^{2+} ion. The bands in the visible region are generally assigned also to ligand field transitions; however, the extended Hückel results predict a variety of ligand → metal charge-transfer transitions through which significant intensity enhancement would occur. Of these ligand → metal charge-transfer transitions, the orbitals of the sulfur ligands are responsible for absorption intensity in the visible region while the orbitals of the sulfur and nitrogen ligands account for absorption intensity in the near-ultraviolet. There is excellent agreement between the observed spectra of these complexes and that predicted by theory with respect to both relative intensity and energy of charge-transfer transitions in the visible and near-ultraviolet regions, and the spectra of the Co^{2+}-enzyme can be accounted for by a chromophore of *accidental* axial symmetry in which the symmetry (z) axis bisects the S-Co-S valence angle of the active site metal ion complex. The agreement between predicted spectra calculated on the basis of molecular orbital models and the observed polarized absorption spectra provide a basis to extend this approach to the study of other small molecule Co^{2+} complexes and Co^{2+}-reconstituted metalloenzymes and to characterize the active site metal ion in inhibitor complexes and reaction intermediates of liver alcohol dehydrogenase.

In a variety of Zn^{2+}-containing metalloenzymes, the catalytically required tetracoordinate metal ion can be replaced by Co^{2+}, often with complete retention of enzymatic activity.[2-4] To probe metal ion function in these enzymes, the coordination structure and the intense electronic absorption properties of Co^{2+} substitutionally incorporated into these enzymes have been an active focus of a large number of spectroscopic studies. Since most of these studies

[†] The University of Chicago, Department of Biochemistry and Molecular Biology.
[‡] Universität des Saarlandes.
[⊥] The University of Chicago, Department of Chemistry.

(1) (a) This work was supported by grants of the NIH (AA 06374), NSF (PCM 77-13479), and the American Heart Association (77873) awarded to M.W.M., a grant of the Deutscheforschungsgemeinschaft awarded to M.Z., and a grant of the NSF (DMR 80-19741) awarded to J.K.B. (b) Established Investigator of the American Heart Association for part of the tenure of this investigation.
(2) Lindskog, S. *Struct. Bonding (Berlin)* **1970**, *8*, 153-196.

0002-7863/87/1509-4072$01.50/0